

A domain adaptation approach in fault detection and isolation of ultrasound sea altimeters

Vito Antonio Nardi
DIIES Department

Università Mediterranea di Reggio Calabria
Reggio Calabria, Italy
vito.nardi@unirc.it
0000-0001-7791-3164

Federico Casella
DICEAM Department

Università Mediterranea di Reggio Calabria
Reggio Calabria, Italy
federico.casella@unirc.it

Mariacarla Lugarà
DIIES Department

Università Mediterranea di Reggio Calabria
Reggio Calabria, Italy
mariacarla.lugara@unirc.it

Valerio Scordamaglia
DIIES Department

Università Mediterranea di Reggio Calabria
Reggio Calabria, Italy
valerio.scordamaglia@unirc.it

Claudio De Capua
DIIES Department

Università Mediterranea di Reggio Calabria
Reggio Calabria, Italy
decapua@unirc.it

Pasquale Filianoti
DICEAM Department

Università Mediterranea di Reggio Calabria
Reggio Calabria, Italy
filianoti@unirc.it

Abstract—This work proposes an approach for the fault detection (FD) of a single out-of-water ultrasound range meter for the measurement of sea height. Although they provide high-frequency and accurate measurements, such sensors are prone to faults, and the presence of foam on the water surface can hinder their measurement capabilities. In contrast, underwater pressure sensors provide more reliable but less accurate measurements of wave characteristics. Furthermore, wave attenuation below the sea surface affects the accuracy of pressure sensors-based measurements of wave motion. This work introduces a procedure for performing transfer learning, aimed at leveraging knowledge acquired from pressure sensor data to train a neural network that provides fault detection capabilities in ultrasonic measurement of sea level. The proposed transfer learning procedure takes advantage of linear wave theory, a description of the motion of small amplitude sea waves, to perform domain adaptation. The effectiveness of the proposed approach is discussed through simulations on a real-world dataset in which three common types of faults are injected.

Index Terms—domain adaptation, fault detection, sea altimeters, pressure transducers, neural networks

I. INTRODUCTION

The scope of this work is to provide a fault detection approach that can be used to detect faults in ultrasound sea altimeters. Sensor fault detection consists of the crucial task of detecting whether a sensor is subject to faults, and thus the data it generates satisfy the specifications of the sensor in terms of accuracy and precision. This task is of importance for almost any field in engineering, such as, for example, robotics [1]–[6], autonomous vehicles [7], power production and management [8], [9], aeronautics [10], and several other fields. Fault detection has been historically based upon sensors redundancy, often relying upon vote-like strategies for performing, also, the task of identifying and isolating the faulty sensor: comparing the output of two sensors performing the same task allows fault detection, while an odd number of sensors allows to identify a faulty sensor whose output significantly differs from the one

of the *majority* of sensors. However, the drawback of this approach lies in multiplying the costs, energy consumption, weight, space, and overall requirements of installing a single sensor.

Fault detection approaches can be broadly classified into model-based and pattern-based ones. In the first category, the output of a sensor is compared against the forecast of a model, if their difference (often called *residual*) exceeds a certain threshold, a fault is detected. In the second one, instead, patterns explicitly associated with faulty or non-faulty conditions are evaluated. Model-based approaches show good performances both in terms of robustness and computational effort, they include parity space solutions, observers, set membership methods, and more (see [11] for a review). However, model-based solutions require a model of the system, which can often require the knowledge of unknown or varying parameters.

Pattern-based solutions rely upon certain statistical characteristics of sensors outputs and they include morphological filtering [12], outlier detection through embedding non-faulty data into a high-dimensional hypersphere [13], fuzzy logic and neural networks [14]. Overall, such approaches, artificial intelligence solutions, and machine learning FD techniques in particular, have been attracting the interest of both the scientific and practitioners communities.

Both the two main approaches in machine learning have been successfully used in fault detection, supervised learning solutions require a dataset of labeled data (i.e., of both faulty and non-faulty data) to train a classifier, such as support vector machine (SVM) [15] and k -nearest neighbors classifiers (kNN), often embedding preprocessing techniques such as principal component analysis (PCA). In unsupervised learning, instead, no labeled datasets are required, although larger ones are usually needed. Recent years have witnessed the rise of deep learning algorithms as the forerunners in machine

learning solutions. Deep learning algorithms are based on increasing complex (*deep*) neural networks that, at the beginning, mimicked the characteristics and capabilities of *natural* neurons. Deep learning algorithms are characterized by a significant number of layers whose stack can be combined to perform complex tasks. Although generally characterized by high training computational costs, deep learning algorithms show good performance in analyzing and reproducing time series.

Fault detection is crucial to ensuring the reliability of monitoring campaigns in particularly challenging environments, such as at sea, where sensor operating conditions are demanding and maintenance operations are both difficult and costly. The precise monitoring of wave motion is important for oceanographic, coastal engineering, and climatic purposes. Two types of sensors are commonly used for water level measurements: pressure sensors [16] and noncontact distance meters [16]–[18]. Water level detection with non-contact sensors has the advantage that the instrument is not directly exposed to water, which makes it more resistant to corrosion effects [19]. Ultrasonic sensors are usually deployed in the direct measurement of the free surface as well as the wave characteristics (wave heights, periods, directions) (e.g., [20]). They operate by generating a pulse or a series of pulses in the ultrasound range and measuring the time it takes for the pulses to be detected by the device’s receiver, typically a piezoelectric transducer [19], [21]. This solution has some critical aspects, since ultrasonic systems to work properly need to be installed at a precise angle (90° with respect to the surface to be detected), so as to receive the echoes reflected by the water surface. In presence of a surface slope or foam, that scattered the signal, there will be frequently missing echoes, which would degrade the measures. Moreover, this type of sensor must be frequently monitored because of the creation of patinas or condensation that could alter its correct functioning. In contrast, pressure sensors measure the variable pressure caused by freely passing waves and are commonly used to study fluid-structure interaction problems (e.g., [22], [23]). Although they offer fast response times, high precision, and durability, they are less effective in capturing wave characteristics related to wind interaction or pure wind waves. This limitation arises because higher frequency components are attenuated during transmission through seawater.

However, both types of sensor face performance limitations when exposed to the harsh marine environment, which introduces operational challenges and potential measurement inaccuracies (e.g., the growth of marine biofouling). Using alarm thresholds or other naive approaches require not always available knowledge of installation characteristics, while using redundant installations indeed increases costs and footprint, both in terms of energy and installation overhead. Quickly replacing faulty sensors allows for the continuity of measurement campaign, while for long-term deployments, a data validation strategy prevents data set from being corrupted by data originating from faulty sensors.

Therefore, a fault detection and data validation strategy is

useful in such measurements. In the literature, only a handful of works deal with such a problem. In [24] a data-driven approach is proposed, but for current profilers. Although not aimed at sensor fault detection, but rather in simulation, in [25] neural networks show good performance in forecasting wave behavior, while a long and wide campaign of wave measurements is validated in [26] through classical statistical approaches. However, none of these approaches addresses the problem of quasi-real-time fault detection for such sensors.

This work proposes a transfer learning approach, namely a domain adaptation approach, for the fault detection of a single wave height ultrasound sensor. Knowledge transfer is the process of using knowledge gathered through one task to improve another. This process is called in different ways if the domain in which knowledge is acquired and then used differs, or if the tasks performed change or remain the same, namely domain adaptation occurs when the trained model performs the same task across different domains [27]. The inherent advantage of transfer learning is the possibility to increase the data available for training of another task, and it has been successfully used in different fault detection tasks; see [28] and [29]. With respect to the task of interest for this paper, domain adaptation allows the usage of knowledge acquired on a dataset of redundant highly reliable pressure sensors in detecting faults of an ultrasound sea-altimeter, without the need for a labeled dataset of ultrasound sea height measurements. Using redundancy, the healthy pressure data can be identified, while linear wave theory enables domain transformation which eventually is used to perform fault detection in ultrasound wave height sensors.

This paper is structured as follows, Section II describes the characteristics of the measurement structure and the relevant linear wave theory. In Section III the fault detection procedure is introduced, along with a brief description of the wave model, the validation of the proposed algorithm is performed in Section IV and its results are briefly discussed in Section V

II. WAVE MEASUREMENT

A deep understanding of wave motion characteristics is crucial for various applications, including assessing the performance of wave energy converters and predicting the impact of waves on maritime structures. Additionally, integrating these parameters with meteorological data—particularly wind speed and direction—using sensor data fusion techniques can support the development of new forecasting models. To advance these objectives, a long-term data acquisition campaign was carried out in 2024 in the marine area off the Marine Energy Laboratory of the University of Reggio Calabria, on the eastern coast of the Strait of Messina. The dataset used for training the neural network was derived from this experimental campaign [30]. Notice that although this experimental setup has a duplex architecture, the aim of this work is tackling fault detection in single-sensor installations.

The experimental setup involved a structure consisting of an iron frame that supports two pressure transducers (ATM.1ST

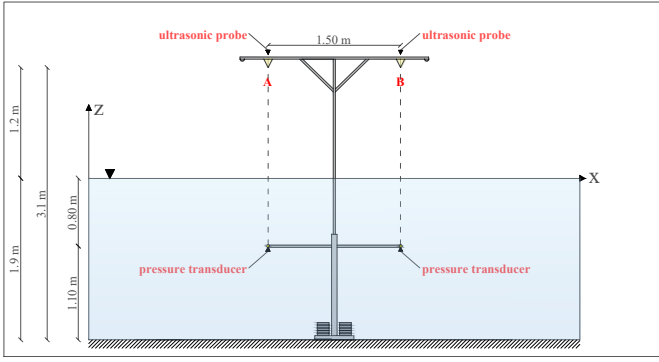


Fig. 1. 2D sketch of the measurement system.

/ N) placed 0.8 m below the free surface, isolated from the seabed, at a depth of water of 1.9 m. This is used to detect the pressure induced by the wave motion. To reconstruct the free-surface profile, two ultrasonic probes (ATG-IRU-2003) were mounted on top at 1.2 m above sea level, 1.5 m from each other (see Fig. 1). The pressure sensors, based on piezoresistive technology, provided an accuracy of $<0.2\%$ FS (full-scale) and a response time of <1 ms. Ultrasonic sensors, which measured wave elevation through sound pulse reflection, had an accuracy of $\pm 0.25\%$ and a response time of 55 ms at 7.62 m. Sensor data were acquired using a National Instruments cDAQ-9185 chassis with two NI-9203 modules, enabling the collection of 4–20 mA output signals. The system was designed for precise, synchronized, and remote data acquisition. To reduce the error due to digital-to-analog conversion, the data were oversampled at 500 Hz and then averaged to reduce the frequency to 10 Hz. Data acquisition was continuous. Each test was identified by a packet of 3,000 samples, corresponding to a duration of 5 minutes. This is because, as stated by [20] this duration is optimal for representing a stationary, Gaussian, sea state. As stated by [31], to reconstruct the free surface from pressure transducer measurements it is common to use the linear wave theory (e.g., [20], [32]). The theory provides a reasonable estimation of the significant wave height but fails to capture the higher-frequency components of the wave spectrum. As a result, it is unable to represent the asymmetrical profile of nonlinear waves and significantly underestimates their crest elevation. However, they are more reliable than ultrasound sensors and their redundancy allows to isolate a dataset of non faulty measurement. For this reason, the data from pressure sensors will be used in this work in performing a domain adaptation approach in fault detection and isolation of the more valuable (yet less reliable) ultrasound sea altimeters.

From this theory, taking into account the dynamic pressure Δ_p (the pressure excluding the static contribution corresponding to the mean level) we can write

$$\Delta_p = \rho g \eta \frac{\cosh(k(z+h))}{\cosh(kh)} \quad (1)$$

where ρ is the density of the fluid, g is the acceleration of gravity, η is the wave profile, k is the wave number, z is

the submersion depth (of the pressure transducer), measured upwards from the still water level and h is the water depth. It is common to re-write Eq.1 as

$$\Delta_p = \rho g \eta K_p \quad (2)$$

where K_p is the attenuation factor (e.g., [20]). By calculating K_p , it is possible to reconstruct the surface spectrum from the pressure wave spectrum. However, this reconstruction is only feasible for a band around the peak frequency, and components at higher frequencies are not present, as they are strongly attenuated during propagation. However, the information obtained can still be used to support the evaluation of the operating status of the ultrasound system.

III. FAULT DETECTION PROCEDURE

Starting as a generalization of principal component analysis, with the seminal work of 1982 by Oja [33], autoencoders gained popularity as a simple yet powerful tool which can efficiently find a lower-dimensional representation of a set of data (*encoding*). This representation can later be used to reproduce (*decode*) data from the encoded representation. In general, the training process in autoencoders relies on performing the encoding/decoding process by minimizing the error (usually mean square error) between the decoded and training data.

Of the several autoencoder architectures that are present in the literature (the interested reader can refer to [34] for a survey), in this work the following 1D CNN (one-dimensional convolutional neural network) structure (which is summarized in Figure 2) is used:

- a sequence input layer which performs z-score normalization (standardization) of data;
- the downsampling layers performing dimensionality reduction, each block formed by a 1-D convolution layer, followed by rectifier or ReLU (rectified linear unit) activation function, then by a dropout layer to prevent overfitting;
- the upsampling layers, which reverse the downsampling through fractionally-strided convolution (see [35]) and embed both the ReLU activation function and a dropout layer;
- the transposed 1-D convolution layer, which eventually produces the desired output.

For the purposes of this work, three downsampling/upsampling layers have been used, following a trial-and-error procedure resulting in a twenty-layer network. The training process uses adaptive momentum estimation (ADAM) with a constant learning rate. The loss function is the mean square error (MSE) between the input and output data sequences.

An example of ultrasound signal reconstruction with and without domain adaptation is reported in Figure 3.

Let introduce the input sequence X_p^k of pressure data at time instant k , and let introduce its autoencoder-forecast $\tilde{X}_p^k =$

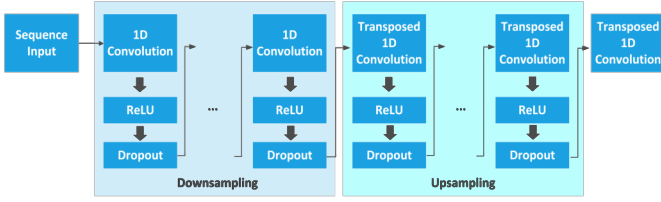


Fig. 2. A schematic of the neural network used in this work.

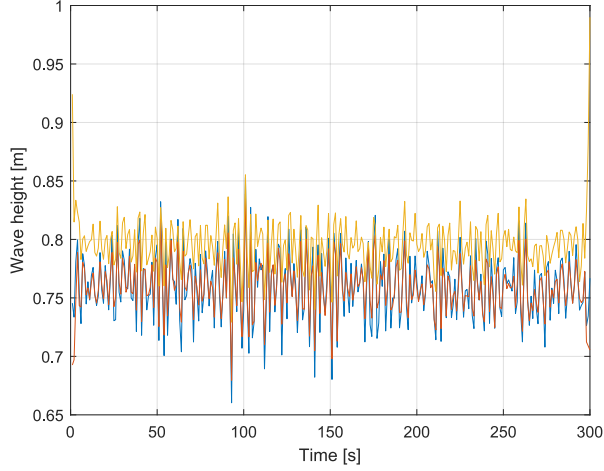


Fig. 3. An example of the original (blue line) and its reconstruction without domain adaptation (orange line) and using the proposed approach (red line), which shows a better accuracy.

$f(X_p^k)$. Let introduce X_k^u as ultrasound-measured data at the same time instant.

Using the model described in II, let introduce \tilde{X}_k^u the forecast of X_k^u as

$$\tilde{X}_k^u = k_p f\left(\frac{1}{k_p} X_k^u\right) \quad (3)$$

with $k_p = \frac{\cos(k(z+h))}{\cosh(kh)}$. Fault detection is performed by evaluating the mean percentage error (MPE) between \tilde{X}_k^u and X_k^u , each time it exceeds a threshold $\tau > 0$ a fault is detected, singularity of MPE when estimate approaches zero is prevented properly capping its value to 100.

IV. VALIDATION

In order to discuss the effectiveness of the proposed approach, a series of tests has been performed and its results are reported in this section.

A. Training and parameter choice

The training data set consists of 68751000 samples (the samples make up 22917 sea states), sampled at 10 Hz of two pressure sensors, the duplex architecture does not allow for a labeling of faulty data, while non-faulty data can be labeled (when the outputs of both sensors differ by a small threshold). Training has been performed with the classic 9:1

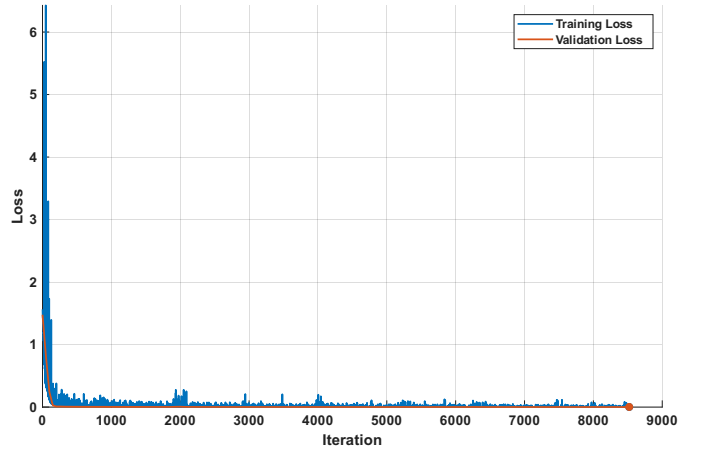


Fig. 4. The training process for the autoencoder used in this work.

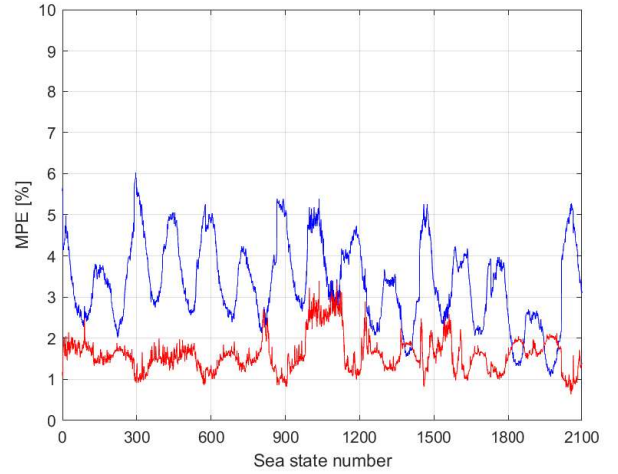


Fig. 5. A comparison of the MPE with (red line) and without (blue line) domain adaptation, in absence of faults.

division between training and validation data, training has been performed for 200 epochs, with a 0.001 learning rate and a 0.2 dropout rate. Training details are reported in Figure 4

As a preliminary investigation step, Figure 5 shows a comparison of the MPE for 2100 sea states in absence of faults. The blue line shows the MPE between autoencoder forecast without domain adaptation, while the red line shows the MPE in the presence of domain adaptation, which reduces the spikes which can lead to false detection of faults. For the whole dataset, the maximum MPE is 6.52% without performing domain adaptation, reduced to 3.93% following the transfer learning procedure. By performing a clustering operation on the dataset, the τ threshold has been set to 3.2%. This value has been set to maximize the accuracy in classification; it is interesting to note that performing the same operation with different clustering weights (see [36] for more details) can maximize either the specificity or the sensitivity of the algorithm.

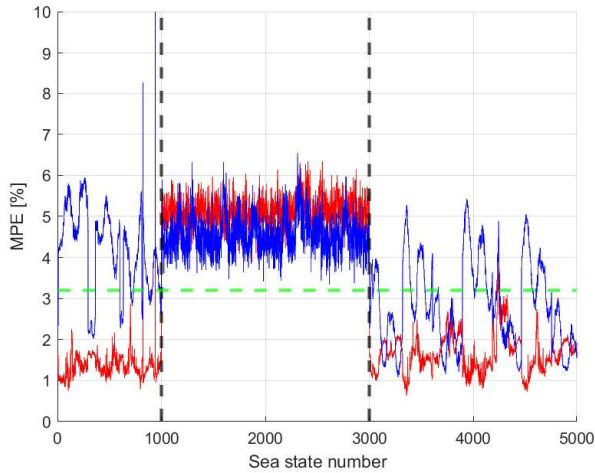


Fig. 6. First fault scenario: an additive white noise is added to sea states from 1000 to 3000 (highlighted by vertical dashed lines), blue line denote the MPE of sea state estimations without transfer learning, while red line denotes transfer learning-enhanced estimation.

	Zeroing fault	Noisy fault	Sinusoidal fault
False positive rate	0.20%	1.05%	0.20%
False negative rate	0.05%	0.05%	2.45%

TABLE I

FALSE POSITIVE AND FALSE NEGATIVE RATES DURING DIFFERENT TESTS.

B. Fault scenarios tests

Figures 6, 7 and 8 represent three fault scenarios, in which an additive disturbance has been added to non faulty data. Three common faults are injected into the dataset, which is described in this section:

- 1) the sensor noise increases (i.e. due to sensor wearing or the presence of sea foam), thus a white noise is summed to the output of the sensor (Figure 6);
- 2) the physical connection to the sensor is cut - this results in the sensor output suddenly becoming 0 (Figure 7);
- 3) a slow frequency ($1/75Hz$) sinusoidal disturbance is added to the output of the sensor (Figure 8), representing slow changes in sea height (i.e. tidal effects) which can vary across different sites of installation.

False positive and false negative rates are reported in Table I. For the first fault scenario (Figure 6) another comparison is performed: the MPE for the sea state estimation with and without domain adaptation is represented (by red and blue lines, respectively). It can be observed that while the injected fault is correctly found in both cases (i.e. MPE is more than the $\tau = 3.2\%$ threshold) in absence of domain adaptation the fault detection process is quite less specific, going beyond the 3.2% threshold in absence of faults.

A brief evaluation of computational cost has been performed, training required roughly twelve minutes on a Xeon-based workstation, while fault detection required roughly 0.004 seconds for each sea state, proving the suitability of the proposed approach in real-time FD.

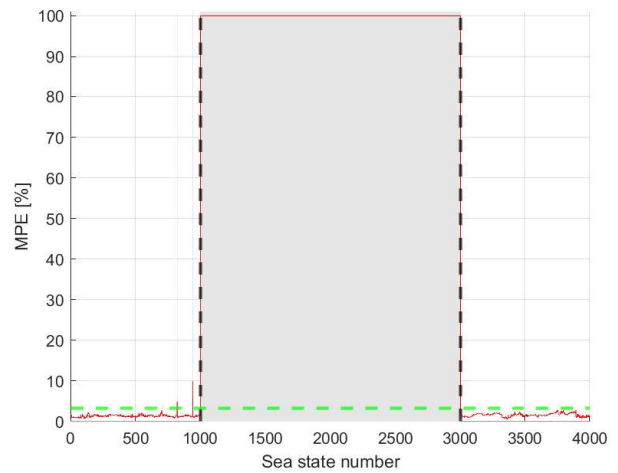


Fig. 7. Second fault scenario: the output of the ultrasound sensors suddenly becomes to zero for sea states from 1000 to 3000, gray area denotes the sea states for which a fault is detected.

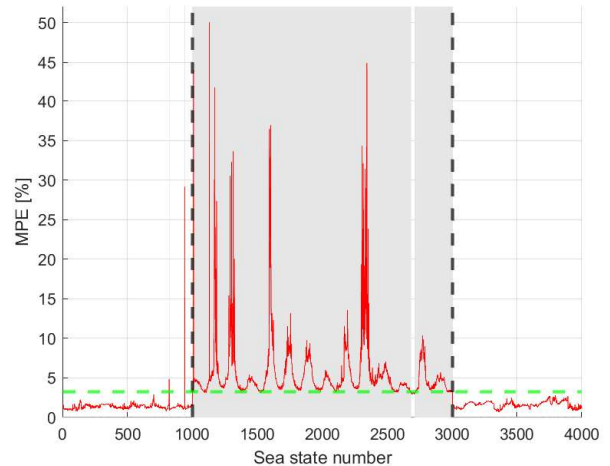


Fig. 8. Third fault scenario: a low-frequency disturbance is added to the sea states from 1000 to 3000, gray area denotes the sea states for which a fault is detected.

V. RESULTS DISCUSSION AND CONCLUSIONS

This work proposes a fault detection approach for ultrasound sensors used in measuring sea waves. Such sensors provide highly valuable data, but are affected by low reliability and are prone to failures due to the harsh marine environment. Thus, the possibility of improving such sensors with fault detection capabilities appears to be of interest. In this work a data set gathered from a duplex installation of the more reliable underwater pressure sensors has been used to train an autoencoder, which is then used for performing fault detection in ultrasound sensors through domain adaptation, by evaluating the mean percentage error (MPE) between autoencoder forecast of sea states and actual measurements. The proposed domain adaptation approach relies upon the linear wave theory and, in the future, the usage of other

wave models will be investigated. It must be noted that the proposed approach produces a fault detection system which is not bound to a specific site, given that the training set is diverse enough. A comparison between sea state MPE with and without domain adaptation has been performed, showing a reduction in maximum MPE from 6.52% to 3.93%, while significantly reducing the false positive detection rate. Further tests performed by injecting faults in real-world data prove the effectiveness of the proposed approach in detecting faults belonging to three common cases.

REFERENCES

- [1] E. Khalastchi and M. Kalech, "Fault detection and diagnosis in multi-robot systems: A survey," *Sensors*, vol. 19, no. 18, p. 4019, 2019.
- [2] A. Ferraro, C. De Capua, and V. Scordamaglia, "Integrated trajectory planning and fault detection for a skid-steered mobile robot deployed in post-disaster scenarios," 11 2024, pp. 413–418.
- [3] A. Ferraro, V. Nardi, E. D'Amato, I. Notaro, and V. Scordamaglia, "Multi-drone systems for search and rescue operations: problems, technical solutions and open issues," in *2023 IEEE International Workshop on Technologies for Defense and Security (TechDefense)*. IEEE, 2023, pp. 159–164.
- [4] E. D'Amato, V. A. Nardi, I. Notaro, and V. Scordamaglia, "A visibility graph approach for path planning and real-time collision avoidance on maritime unmanned systems," in *2021 International Workshop on Metrology for the Sea; Learning to Measure Sea Health Parameters (MetroSea)*. IEEE, 2021, pp. 400–405.
- [5] V. Scordamaglia, A. Ferraro, F. Tedesco, and G. Franzè, "Set-theoretic approach for autonomous tracked vehicles involved in post-disaster first relief operations," in *2024 10th International Conference on Control, Decision and Information Technologies (CoDIT)*. IEEE, 2024, pp. 2006–2011.
- [6] A. Ferraro and V. Scordamaglia, "Coordinated trajectory planning for ground-based multi-robot systems in exploration and surveillance missions," in *2023 IEEE International Workshop on Technologies for Defense and Security (TechDefense)*. IEEE, 2023, pp. 131–136.
- [7] J. Lee, K. Oh, Y. Yoon, T. Song, T. Lee, and K. Yi, "Adaptive fault detection and emergency control of autonomous vehicles for fail-safe systems using a sliding mode approach," *IEEE Access*, vol. 10, pp. 27 863–27 880, 2022.
- [8] H. Henao, G.-A. Capolino, M. Fernandez-Cabanas, F. Filippetti, C. Bruzzese, E. Strangas, R. Pusca, J. Estima, M. Riera-Guasp, and S. Hedayati-Kia, "Trends in fault diagnosis for electrical machines: A review of diagnostic techniques," *IEEE industrial electronics magazine*, vol. 8, no. 2, pp. 31–42, 2014.
- [9] G. Fulco, F. Ruffa, M. Lugarà, P. Filianoti, and C. De Capua, "Automatic station for monitoring a microgrid," in *Proceedings of the 24th IMEKO TC4 International Symposium and 22nd International Workshop on ADC and DAC Modelling and Testing, Palermo, Italy, 2022*, pp. 14–16.
- [10] C. Hajiyev and F. Caliskan, *Fault diagnosis and reconfiguration in flight control systems*. Springer Science & Business Media, 2003, vol. 2.
- [11] S. X. Ding, *Model-based fault diagnosis techniques: design schemes, algorithms, and tools*. Springer Science & Business Media, 2013.
- [12] H. Li and D. Yun Xiao, "Fault diagnosis using pattern classification based on one-dimensional adaptive rank-order morphological filter," *Journal of Process Control*, vol. 22, no. 2, pp. 436–449, 2012. [Online]. Available: <https://www.sciencedirect.com/science/article/pii/S0959152411002423>
- [13] Z. Yang, X. Fu, W. Jin, L. Yuehong, and W. Shengwei, "A robust pattern recognition-based fault detection and diagnosis (fdd) method for chillers," *HVAC&R Research*, vol. 20, no. 7, pp. 798–809, 2014. [Online]. Available: <https://doi.org/10.1080/10789669.2014.938006>
- [14] B. K. Ponukumati, P. Sinha, M. K. Maharana, C. Jenab, A. V. Pavan Kumar, and K. Akkenaguntla, "Pattern recognition technique based fault detection in multi-microgrid," in *2021 IEEE 2nd International Conference on Applied Electromagnetics, Signal Processing, & Communication (AESPC)*, 2021, pp. 1–6.
- [15] V. A. Nardi, M. Lanza, F. Ruffa, and V. Scordamaglia, "An artificial intelligence approach for the kinodynamically feasible trajectory planning of a car-like vehicle," *Applied Sciences*, vol. 15, no. 2, p. 795, 2025.
- [16] R. Suchitra, K. Ezhilsabareesh, and A. Samad, "Development of a reduced order wave to wire model of an owc wave energy converter for control system analysis," *Ocean Engineering*, vol. 172, pp. 614–628, 2019.
- [17] L. Ciappi, L. Cheli, I. Simonetti, A. Bianchini, L. Talluri, L. Cappi-etti, and G. Manfrida, "Analytical models of oscillating water column systems operating with air turbines in the mediterranean sea," in *Proceedings of the 15th Conference on Sustainable Development of Energy, Water and Environment Systems*, Cologne, Germany, 2020, pp. 1–5.
- [18] R. Mayon, D. Ning, C. Zhang, L. Chen, and R. Wang, "Wave energy capture by an omnidirectional point sink oscillating water column system," *Applied Energy*, vol. 304, p. 117795, 2021.
- [19] L. Cappi-etti, I. Simonetti, V. Penchev, and P. Penchev, "Laboratory tests on an original wave energy converter combining oscillating water column and overtopping devices," in *Advances in Renewable Energies Offshore*, C. Guedes Soares, Ed. London: Taylor & Francis Group, 2018.
- [20] P. Boccotti, *Wave mechanics and wave loads on marine structures*. Butterworth-Heinemann, 2014.
- [21] T. Pereira, T. de Carvalho, T. Mendes, and K. Formiga, "Evaluation of water level in flowing channels using ultrasonic sensors," *Sustainability*, vol. 14, no. 9, p. 5512, 2022.
- [22] G. Tripepi, F. Aristodemo, D. D. Meringolo, L. Gurnari, and P. Filianoti, "Hydrodynamic forces induced by a solitary wave interacting with a submerged square barrier: Physical tests and δ -les-sph simulations," *Coastal Engineering*, vol. 158, p. 103690, 2020.
- [23] F. Aristodemo and P. Filianoti, "On the stability of submerged rigid breakwaters against solitary waves," *Coastal Engineering*, vol. 177, p. 104196, 2022.
- [24] V. Scordamaglia, A. Ferraro, L. Gurnari, F. Ruffa, C. De Capua, and P. Giuseppe Filianoti, "A data-driven algorithm for detecting anomalies in underwater sensor-based wave height measurements," in *2023 IEEE International Workshop on Metrology for the Sea; Learning to Measure Sea Health Parameters (MetroSea)*, 2023, pp. 21–26.
- [25] J. Wang, B. J. Bethel, W. Xie, and C. Dong, "A hybrid model for significant wave height prediction based on an improved empirical wavelet transform decomposition and long-short term memory network," *Ocean Modelling*, vol. 189, p. 102367, 2024. [Online]. Available: <https://www.sciencedirect.com/science/article/pii/S1463500324000544>
- [26] P. Queffelec, "Long-term validation of wave height measurements from altimeters," *Marine Geodesy*, vol. 27, no. 3–4, pp. 495–510, 2004. [Online]. Available: <https://doi.org/10.1080/01490410490883478>
- [27] S. J. Pan and Q. Yang, "A survey on transfer learning," *IEEE Transactions on Knowledge and Data Engineering*, vol. 22, no. 10, pp. 1345–1359, 2010.
- [28] Z. Zhao, Q. Zhang, X. Yu, C. Sun, S. Wang, R. Yan, and X. Chen, "Applications of unsupervised deep transfer learning to intelligent fault diagnosis: A survey and comparative study," *IEEE Transactions on Instrumentation and Measurement*, vol. 70, pp. 1–28, 2021.
- [29] H. Chen, H. Luo, B. Huang, B. Jiang, and O. Kaynak, "Transfer learning-motivated intelligent fault diagnosis designs: A survey, insights, and perspectives," *IEEE Transactions on Neural Networks and Learning Systems*, vol. 35, no. 3, pp. 2969–2983, 2024.
- [30] F. Casella, F. Aristodemo, L. Mariacarla, and P. G. F. Filianoti, "Wind-wave forces on a smooth and rough horizontal submerged cylinder: a field experiment," *Coastal Engineering*, 2025 (in press).
- [31] A. Mouragues, P. Bonneton, D. Lannes, B. Castelle, and V. Marieu, "Field data-based evaluation of methods for recovering surface wave elevation from pressure measurements," *Coastal Engineering*, vol. 150, pp. 147–159, 2019.
- [32] C. T. Bishop and M. A. Donelan, "Measuring waves with pressure transducers," *Coastal Engineering*, vol. 11, no. 4, pp. 309–328, 1987.
- [33] E. Oja, "Simplified neuron model as a principal component analyzer," *Journal of mathematical biology*, vol. 15, pp. 267–273, 1982.
- [34] D. Bank, N. Koenigstein, and R. Giryes, "Autoencoders," *Machine learning for data science handbook: data mining and knowledge discovery handbook*, pp. 353–374, 2023.
- [35] V. Dumoulin and F. Visin, "A guide to convolution arithmetic for deep learning," *arXiv preprint arXiv:1603.07285*, 2016.
- [36] N. Gershenfeld, "Nonlinear inference and cluster-weighted modeling," *Annals of the New York Academy of Sciences*, vol. 808, no. 1, pp. 18–24, 1997. [Online]. Available: <https://nyaspubs.onlinelibrary.wiley.com/doi/abs/10.1111/j.1749-6632.1997.tb51651.x>